

HYPERNOVA NUCLEOSYNTHESIS AND GALACTIC CHEMICAL EVOLUTION

To be published in "The Influence of Binaries on Stellar Population Studies",
ed. D. Vanbeveren (Kluwer), 2001.

Ken'ichi Nomoto, Keiichi Maeda, Hideyuki Umeda
Takayoshi Nakamura

*Department of Astronomy and Research Center for the Early Universe
School of Science, University of Tokyo*

Abstract

We study nucleosynthesis in 'hypernovae', i.e., supernovae with very large explosion energies ($\gtrsim 10^{52}$ ergs) for both spherical and aspherical explosions. The hypernova yields compared to those of ordinary core-collapse supernovae show the following characteristics: 1) Complete Si-burning takes place in more extended region, so that the mass ratio between the complete and incomplete Si burning regions is generally larger in hypernovae than normal supernovae. As a result, higher energy explosions tend to produce larger $[(\text{Zn}, \text{Co})/\text{Fe}]$, small $[(\text{Mn}, \text{Cr})/\text{Fe}]$, and larger $[\text{Fe}/\text{O}]$, which could explain the trend observed in very metal-poor stars. 2) Si-burning takes place in lower density regions, so that the effects of α -rich freezeout is enhanced. Thus ^{44}Ca , ^{48}Ti , and ^{64}Zn are produced more abundantly than in normal supernovae. The large $[(\text{Ti}, \text{Zn})/\text{Fe}]$ ratios observed in very metal poor stars strongly suggest a significant contribution of hypernovae. 3) Oxygen burning also takes place in more extended regions for the larger explosion energy. Then a larger amount of Si, S, Ar, and Ca ("Si") are synthesized, which makes the "Si"/O ratio larger. The abundance pattern of the starburst galaxy M82 may be attributed to hypernova explosions. Asphericity in the explosions strengthens the nucleosynthesis properties of hypernovae except for "Si"/O. We thus suggest that hypernovae make important contribution to the early Galactic (and cosmic) chemical evolution.

1. INTRODUCTION

Massive stars in the range of 8 to $\sim 100M_{\odot}$ undergo core-collapse at the end of their evolution and become Type II and Ib/c supernovae (SNe

II and SNe Ib/c) unless the entire star collapses into a black hole with no mass ejection (e.g., Arnett 1996). These SNe II and SNe Ib/c (as well as Type Ia supernovae) release large explosion energies and eject explosive nucleosynthesis products, thus having strong dynamical, thermal, and chemical influences on the evolution of interstellar matter and galaxies. Therefore, the explosion energies of core-collapse supernovae are fundamentally important quantities. An estimate of $E \sim 1 \times 10^{51}$ ergs has often been used in calculating nucleosynthesis (e.g., Woosley & Weaver 1995; Thielemann et al. 1996) and the impact on the interstellar medium. (In the present paper, we use the explosion energy E for the final kinetic energy of explosion.)

SN1998bw called into question the applicability of the above energy estimate for all core-collapse supernovae. This supernova was discovered in the error box of the gamma-ray burst GRB980425, only 0.9 days after the date of the gamma-ray burst and was very possibly linked to it (Galama et al. 1998). SN1998bw is classified as a Type Ic supernova (SN Ic) but it is quite an unusual supernova. The very broad spectral features and the light curve shape have led to the conclusion that SN 1998bw was a hyper-energetic explosion of a massive ($\sim 14 M_{\odot}$) C + O star with $E = 3 - 6 \times 10^{52}$ ergs, which is about thirty times larger than that of a normal supernova (Iwamoto et al. 1998; Woosley et al. 1999; Branch 2000; Nakamura et al. 2001a). The amount of ^{56}Ni ejected from SN1998bw is found to be $M(^{56}\text{Ni}) \simeq 0.4 - 0.7 M_{\odot}$ (Nakamura et al. 2001a; Sollerman et al. 2000), which is about 10 times larger than the $0.07M_{\odot}$ produced in SN1987A, a typical value for core-collapse supernovae.

In the present paper, we use the term 'Hypernova' to describe such an extremely energetic supernova as $E \gtrsim 10^{52}$ ergs without specifying the nature of the central engine (Nomoto et al. 2000).

Recently, other hypernova candidates have been recognized. SN1997ef and SN1998ey are also classified as SNe Ic, and show very broad spectral features similar to SN1998bw (Iwamoto et al. 2000). The spectra and the light curve of SN1997ef have been well simulated by the explosion of a $10M_{\odot}$ C+O star with $E = 1.0 \pm 0.2 \times 10^{52}$ ergs and $M(^{56}\text{Ni}) \sim 0.15 M_{\odot}$ (Iwamoto et al. 2000; Mazzali, Iwamoto, & Nomoto 2000). SN1997cy is classified as a SN IIn and unusually bright (Germany et al. 2000; Turatto et al. 2000). Its light curve has been simulated by a circumstellar interaction model which requires $E \sim 5 \times 10^{52}$ ergs (Turatto et al. 2000). The spectral similarity of SN1999E to SN1997cy (Cappellaro et al. 1999) would suggest that SN1999E is also a hypernova. Note that all of these estimates of E assume a spherically symmetric event.

Hypernovae may be associated with the formation of a black hole as has been discussed in the context of the GRB-SNe connection (Woosley 1993; Paczynski 1998; Iwamoto et al. 1998; MacFadyen & Woosley 1999). In these models, the gravitational energy, or the rotational energy would be released via pair-neutrino annihilation or the Blandford-Znajek mechanism (Blandford & Znajek 1977). Alternatively, large magnetic energies are released from a possible magnetar (Nakamura 1998; Wheeler et al. 2000). The explosion may also be aspherical (Höflich et al. 1999; MacFadyen & Woosley 1999; Khokhlov et al. 1999).

We investigate the characteristics of nucleosynthesis in such energetic core-collapse hypernovae, the systematic study of which has not yet been done. We examine both spherical and aspherical explosion models and discuss their contributions to the Galactic chemical evolution.

2. SPHERICAL HYPERNOVA EXPLOSIONS

We use various progenitor models with the main sequence masses of 20, 25, 30, and $40M_{\odot}$ (whose He core masses are 6, 8, 10, $16M_{\odot}$, respectively) (Nomoto & Hashimoto 1988; Umeda, Nomoto, & Nakamura 2000), metallicity of $Z = 0$ to solar, and explosion energies of $E_{51} = E/10^{51}$ ergs = 1 - 100 (Nakamura et al. 2001b; Umeda & Nomoto 2001).

In core-collapse supernovae/hypernovae, stellar material undergoes shock heating and subsequent explosive nucleosynthesis. Iron-peak elements including Cr, Mn, Co, and Zn are produced in two distinct regions, which are characterized by the peak temperature, T_{peak} , of the shocked material (Fig. 2). For $T_{\text{peak}} > 5 \times 10^9$ K, material undergoes complete Si burning whose products include Co, Zn, V, and some Cr after radioactive decays. For 4×10^9 K $< T_{\text{peak}} < 5 \times 10^9$ K, incomplete Si burning takes place and its after decay products include Cr and Mn (e.g., Hashimoto, Nomoto, Shigeyama 1989; Woosley & Weaver 1995; Thielemann, Nomoto & Hashimoto 1996).

Figure 1 shows nucleosynthesis in hypernovae and normal supernovae for $E_{51} = 30$ and 1. The progenitor is $40M_{\odot}$ star model (Nakamura et al. 2001b). From this figure, we note the following characteristics of nucleosynthesis with very large explosion energies.

1) The region of complete Si-burning, where ^{56}Ni is dominantly produced, is extended to the outer, lower density region. The large amount of ^{56}Ni observed in hypernovae (e.g., $\sim 0.4 - 0.7 M_{\odot}$ for SN1998bw and $\sim 0.15M_{\odot}$ for SN1997ef) implies that the mass cut is rather deep, so that the elements synthesized in this region such as ^{59}Cu , ^{63}Zn , and ^{64}Ge (which decay into ^{59}Co , ^{63}Cu , and ^{64}Zn , respectively) are ejected more

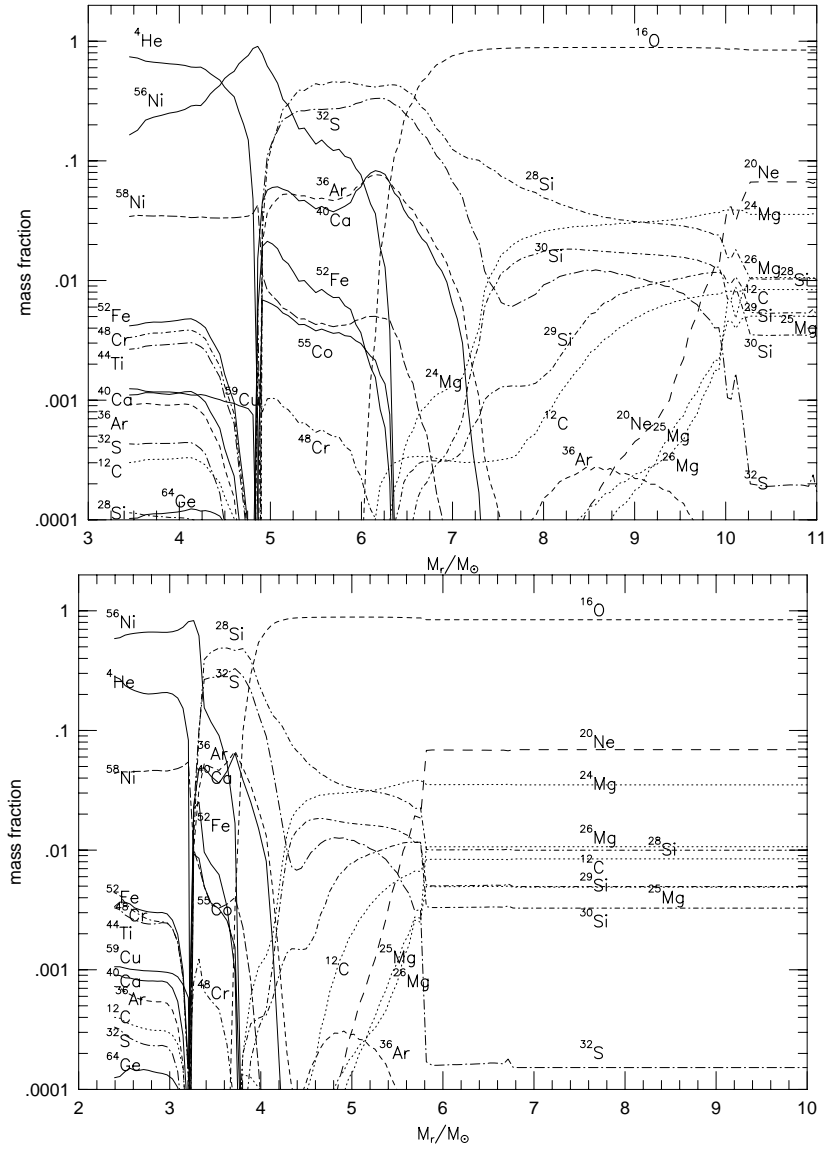


Figure 1 Nucleosynthesis in hypernovae and normal core-collapse supernovae for explosion energies of $E = 30$ (left) and 1 (right) $\times 10^{51}$ ergs. The progenitor model is the $40M_{\odot}$ star model (Nakamura et al. 2001b).

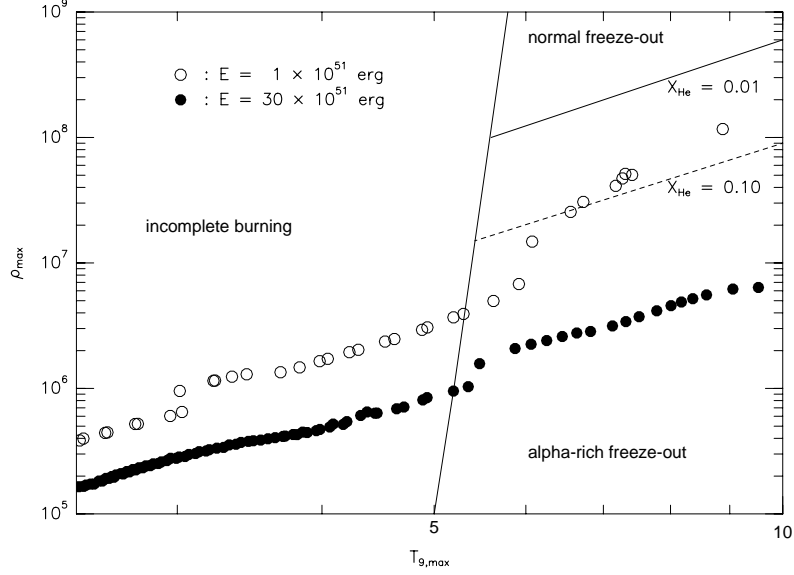


Figure 2 The $\rho - T$ conditions of individual mass zones at their temperature maximum in hypernovae ($E = 30 \times 10^{51}$ ergs: filled circles) and normal supernovae ($E = 1 \times 10^{51}$ erg: open circles) (Nakamura et al. 2001b).

abundantly than in normal supernovae. In the complete Si-burning region of hypernovae, elements produced by α -rich freezeout are enhanced because nucleosynthesis proceeds at lower densities than in normal supernovae (Fig. 2). Figure 1 clearly shows the trend that a larger amount of ${}^4\text{He}$ is left in hypernovae. Hence, elements synthesized through capturing of α -particles, such as ${}^{44}\text{Ti}$, ${}^{48}\text{Cr}$, and ${}^{64}\text{Ge}$ (decaying into ${}^{44}\text{Ca}$, ${}^{48}\text{Ti}$, and ${}^{64}\text{Zn}$, respectively) are more abundant.

2) More energetic explosions form a broader incomplete Si-burning region. The elements produced mainly in this region such as ${}^{52}\text{Fe}$, ${}^{55}\text{Co}$, and ${}^{51}\text{Mn}$ (decaying into ${}^{52}\text{Cr}$, ${}^{55}\text{Mn}$, and ${}^{51}\text{V}$, respectively) are synthesized more abundantly with the larger explosion energy.

3) Oxygen and carbon burning takes place in more extended, lower density regions for the larger explosion energy. Therefore, the elements O, C, Al are burned more efficiently and the abundances of the elements in the ejecta are smaller, while a larger amount of burning products such as Si, S, and Ar is synthesized by oxygen burning.

Nucleosynthesis is characterized by large abundance ratios of intermediate mass nuclei and heavy nuclei with respect to ${}^{56}\text{Fe}$ for more energetic explosions, except for the elements O, C, Al which are consumed in oxygen and carbon burning. In particular, the amounts of ${}^{44}\text{Ca}$ and ${}^{48}\text{Ti}$

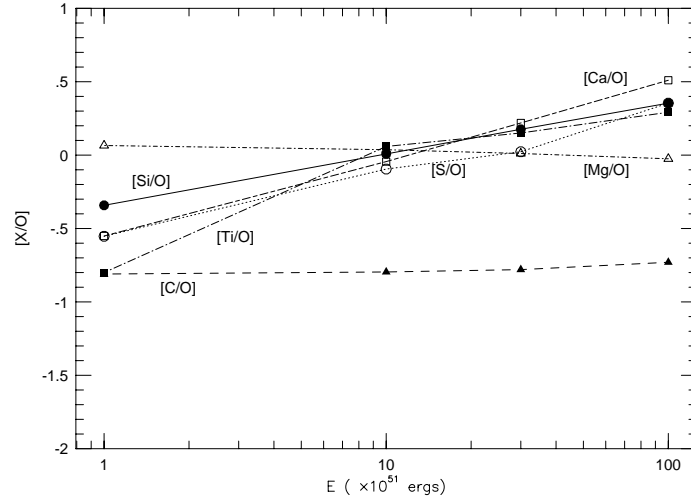


Figure 3 Abundance ratios to oxygen relative to solar values as a function of the explosion energy E . The progenitor model is the $25M_{\odot}$ star model (Nakamura et al. 2001b).

are increased significantly with increasing explosion energy because of the lower density regions which experience complete Si-burning through α -rich freezeout. To see this more clearly, we add the isotopes and show in Figure 3 their ratios to oxygen relative to the solar values for various explosion energies. We note that [C/O] and [Mg/O] are not sensitive to the explosion energy because C, O, and Mg are consumed by oxygen burning. On the other hand, [Si/O], [S/O], [Ti/O], and [Ca/O] are larger for larger explosion energies because Si and S are produced in the oxygen burning region, and Ti and Ca are increased in the enhanced α -rich freezeout.

3. ASPHERICAL EXPLOSIONS

Despite the success of the hypernova model in reproducing the observed features of SN 1998bw at early times, some properties of the observed light curve and spectra at late times are difficult to explain in the context of a spherically symmetric model. (1) The decline of the observed light curve tail is slower than that of the synthetic curve, indicating that at advanced epochs γ -ray trapping is more efficient than expected (Nakamura et al. 2001a; Sollerman et al. 2000). (2) In the nebular epoch, the OI]6300Å emission is narrower than the emission centered at 5200Å. This latter feature can be identified as FeII], although it

may also contain allowed FeII transitions. If the identification is correct, the difference in width may suggest that the mean expansion velocity of iron is higher than that of oxygen and that a significant amount of oxygen exists at low velocity (Danziger et al. 1999; Nomoto et al. 2000; Patat et al. 2001). Both these features are in conflict with what is expected from a spherically symmetric explosion model, where γ -ray deposition is a decreasing function of time and where iron is produced in the deepest layers and thus has a lower average velocity than oxygen. We suggest that these are the signatures of asymmetry in the ejecta. We thus examine aspherical explosion models for hypernovae.

On the theoretical side, MacFadyen & Woosley (1999) showed that the collapse of a rotating massive core can form a black hole with an accretion disk, and that a jet emerges along the rotation axis. The jet can produce a highly asymmetric supernova explosion (Khokhlov et al. 1999). However, these studies did not calculate explosive nucleosynthesis, nor spectroscopic and photometric features of aspherical explosions. Nagataki et al. (1997) performed nucleosynthesis calculations for aspherical supernova explosions to explain some features of SN 1987A, but they only addressed the case of a normal explosion energy.

Maeda et al. (2000) have examined the effect of aspherical (jet-like) explosions on nucleosynthesis in hypernovae. They have investigated the degree of asphericity in the ejecta of SN 1998bw, which is critically important information to confirm the SN/GRB connection, by computing synthetic spectra for the various models viewed from different orientations and comparing the results with the observed late time spectra (Patat et al. 2001).

3.1. NUCLEOSYNTHESIS

Maeda et al. (2000) have constructed several asymmetric explosion models. The progenitor model is the $16 M_{\odot}$ He core of the $40 M_{\odot}$ star. The explosion energy is $E = 1 \times 10^{52}$ ergs.

Figure 4 shows the isotopic composition of the ejecta of asymmetric explosion model in the direction of the jet (upper panel) and perpendicular to it (lower panel). In the z -direction, where the ejecta carry more kinetic energy, the shock is stronger and post-shock temperatures are higher, so that explosive nucleosynthesis takes place in more extended, lower density regions compared with the r -direction. Therefore, larger amounts of α -rich freeze-out elements, such as ^4He and ^{56}Ni (which decays into ^{56}Fe via ^{56}Co) are produced in the z -direction than in the r -direction. Also, the expansion velocity of newly synthesized heavy elements is much higher in the z -direction.

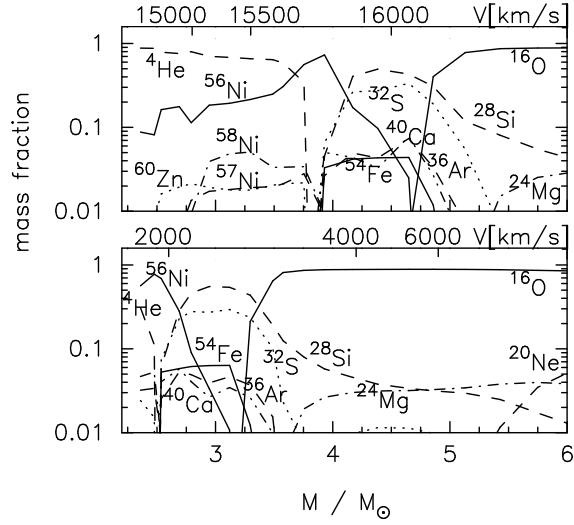


Figure 4 The isotopic composition of the ejecta in the direction of the jet (upper panel) and perpendicular to it (lower panel). The ordinate indicates the initial spherical Lagrangian coordinate (M_r) of the test particles (lower scale), and the final expansion velocities (V) of those particles (upper scale) (Maeda et al. 2000).

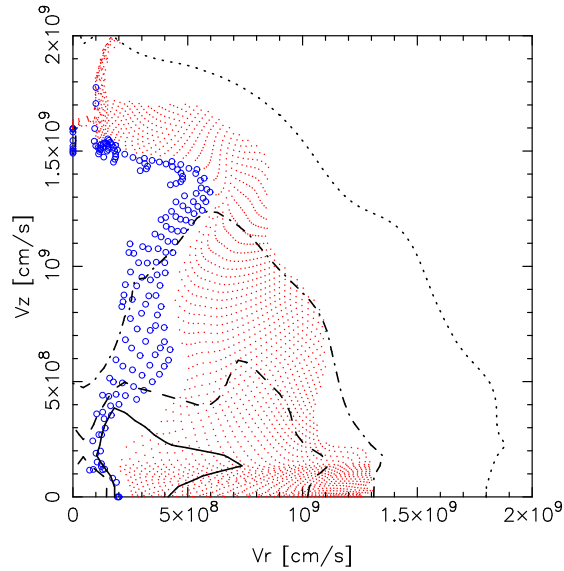


Figure 5 The distribution of ^{56}Ni (open circles) and ^{16}O (dots). The open circles and the dots denote test particles in which the mass fraction of ^{56}Ni and ^{16}O , respectively, exceeds 0.1. The lines are density contours at the level of 0.5 (solid), 0.3 (dashed), 0.1 (dash-dotted), and 0.01 (dotted) of the max density, respectively (Maeda et al. 2000).

Comparison with the nucleosynthesis of spherically symmetric hypernova explosions (Nakamura et al. 2001b) shows that the distribution and expansion velocity of newly synthesized elements ejected in the z -direction is similar to the result of the spherical explosion model with $E \sim 3 \times 10^{52}$ ergs, although the integrated kinetic energy is only $E = 1 \times 10^{52}$ ergs.

On the other hand, along the r -direction ^{56}Ni is produced only in the deepest layers, and the elements ejected in this direction are mostly the products of hydrostatic nuclear burning stages (O) with some explosive oxygen-burning products (Si, S, etc). The expansion velocities are much lower than in the z -direction.

Figure 5 shows the 2D distribution of ^{56}Ni and ^{16}O in the homologous expansion phase. In the direction closer to the z -axis, the shock is stronger and a low density, ^4He -rich region is produced. ^{56}Ni is distributed preferentially in the jet direction. The distribution of heavy elements is elongated in the z -direction, while the ^{16}O distribution is less aspherical.

3.2. NEBULA SPECTRA OF SN 1998BW

Mazzali et al. (2001) calculated synthetic nebular-phase spectra of SN 1998bw using a spherically symmetric NLTE nebular code, based on the deposition of γ -rays from ^{56}Co decay in a nebula of uniform density and composition. They showed that the nebular lines of different elements can be reproduced if different velocities are assumed for these elements, and that a significant amount of slowly-moving O is necessary to explain the zero velocity peak of the O I] line. Different amounts of ^{56}Ni ($0.35M_{\odot}$ and $0.6M_{\odot}$, respectively) are required to fit the narrow O I] line and the broad-line Fe spectrum (see figures in Danziger et al. 1999 and Nomoto et al. 2000). This suggests that an aspherical distribution of Fe and O may explain the observations.

In order to verify the observable consequences of an axisymmetric explosion, we calculated the profiles of the Fe-dominated blend near 5200\AA , and of O I] $6300, 6363\text{\AA}$. These are the lines that deviate most from the expectations from a spherically symmetric explosion. Line emissivities were obtained from the 1D NLTE code, and the column densities of the various elements along different lines of sight were derived from the element distribution obtained from our 2D explosion models.

The nebular line profiles of iron and oxygen with various view angles are shown in Figure 6 together with the spherical model (Maeda 2001). In this figure, the observed spectrum on day 139 (Patat et al. 2001) is also plotted for comparison.

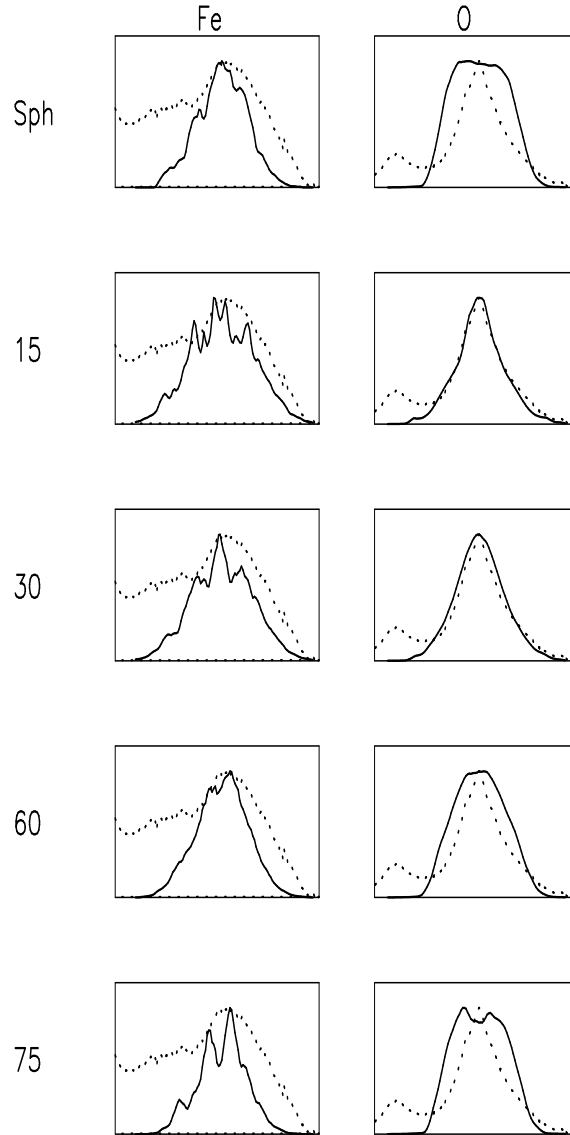


Figure 6 The profiles of the Fe-blend (left panels) and of O I] 6300, 6363 Å (right panels) viewed at 15°, 30°, 60° and 75° from the jet direction (Maeda 2001). The top panel shows the profiles of the spherically symmetric model. The observed lines at a SN rest-frame epoch of 139 days are also plotted for comparison (dotted lines, Patat et al. 2000). The intensities of the strongest lines, normalized to O I] 6300.3Å are: FeII 5158.8Å: 0.207; FeII 5220.1Å: 0.043; FeII 5261.6Å: 0.139; FeII 5273.3Å: 0.066; FeII 5333.6Å: 0.099; FeIII 5270.4Å: 0.086; and OI 6363.8Å: 0.331.

The ‘full-width-at-half-maximum’ of our synthetic lines should be compared to the observational values, which are 440Å for the Fe-blend and 200Å for the O I] doublet, and were estimated from the late time spectrum of 12 Sept 1998, 139 days after the explosion in the SN rest frame, assuming that the continuum level is the value around 5700 Å where the flux has the minimum value.

The observed line profiles are not explained with a spherical model. In a spherical explosion, oxygen is located at higher velocities than iron, and although the Fe-blend can be wider than the O line if the O and Fe regions are mixed extensively, the expected ratio of the width of the Fe-blend and the O line even in fully mixed model is $\sim 3 : 2$ (Mazzali et al. 2001). However, the observed ratio is even larger, $\sim 2 : 1$.

Because Fe is distributed preferentially along the jet direction, our aspherical explosion models can produce a larger ratio. If we view the aspherical explosion model from a near-jet direction, the ratio between the Fe and O line widths is comparable to the observed value. For a larger explosion energy, the width of the oxygen line is too large to be compatible with the observations.

The aspherical explosion models can produce a larger ratio than the spherical model because Fe is distributed preferentially along the jet direction. If the explosion energy is too large, the width of the oxygen line is too large to be compatible with the observations.

The iron and oxygen profiles viewed at an angle of 15° from the jet direction are compared to the observed spectrum on day 139 in Figure 6. When the degree of asphericity is high and the viewing angle is close to the jet direction, the component iron lines in the blend have double-peaked profiles, the blue- and red-shifted peaks corresponding to Fe-dominated matter moving towards and away from us, respectively. This is because Fe is produced mostly along the z (jet) direction. Because of the high velocity of Fe, the peaks are widely separated, making the blend wide. This is the case for the synthetic Fe-blend shown in Figure 6. In contrast, the oxygen line is narrower and has a sharper peak, because O is produced mostly in the r -direction, at lower velocities and with a less aspherical distribution.

The Fe-blend line computed with the aspherical model shows some small peaks (Fig. 6), which are not seen in the observations. However, the detailed profile of the Fe-blend is very sensitive to the matter distribution. Mixing of the ejecta may distribute the fast-moving ^{56}Ni to lower velocities, which would reduce the double-peaked profiles of the Fe lines.

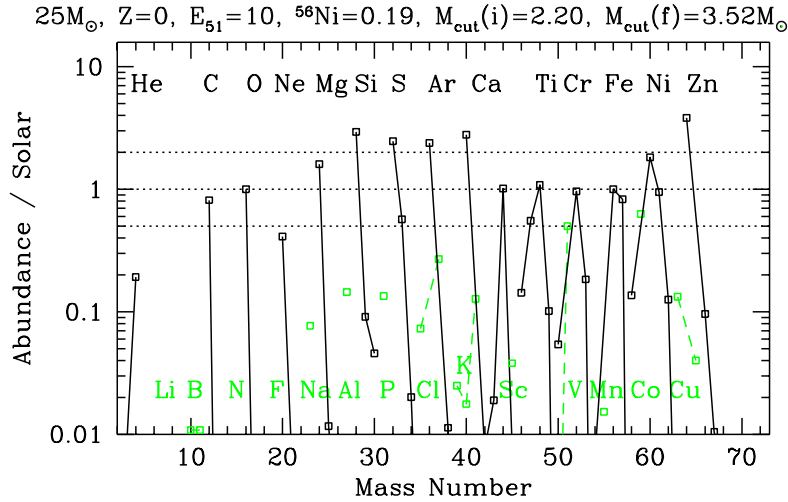


Figure 7 Abundance pattern in the ejecta normalized by the solar ^{16}O abundances for the $25M_{\odot}$ model with $E_{51} = 10$. The mass-cuts are chosen to give large $[\text{Zn}/\text{Fe}]$ and $[\text{O}/\text{Fe}] = 0$ (Umeda & Nomoto 2001).

4. CONTRIBUTION OF HYPERNOVAE TO THE GALACTIC CHEMICAL EVOLUTION

The abundance pattern of metal-poor stars with $[\text{Fe}/\text{H}] < -2$ provides us with very important information on the formation, evolution, and explosions of massive stars in the early evolution of the galaxy. Contributions of hypernova nucleosynthesis to the Galactic chemical evolution could be important because of their large amounts of heavy elements production. Figure 7 shows the abundance pattern of the explosion of the Pop III (metal-free) $25 M_{\odot}$ star.

If hypernovae occurred in the early stage of the Galactic evolution, the abundance pattern of a hypernova may be observable in some low-mass halo stars. This results from the very metal-poor environment, where the heavy elements synthesized in a single hypernova (or a single supernova) dominate the heavy element abundance pattern (Audouze & Silk 1995). It is plausible that hypernova explosions induce star formations. The low-mass stars produced by this event should have the hypernova-like abundance pattern and still exist in the Galactic halo. The metallicity of such stars is likely to be determined by the ratio of ejected iron mass from the relevant hypernova to the mass of hydrogen gathered by the hypernova, which might be in the range range of $-4 \lesssim [\text{Fe}/\text{H}] \lesssim -2.5$

(Ryan et al. 1996; Shigeyama & Tsujimoto 1998; Nakamura et al. 1999; Argast et al. 2000).

4.1. IRON, TITANIUM

One of the most significant features of hypernova nucleosynthesis is a large amount of Fe. One hypernova can produce 2 - 10 times more Fe than normal core-collapse supernovae, which is almost the same amount of Fe as produced in a SN Ia. This large iron production leads to small ratios of α elements over iron in hypernovae (Figure 7). In this connection, the abundance pattern of the very metal-poor binary CS22873-139 ($[\text{Fe}/\text{H}] = -3.4$) is interesting. This binary has only an upper limit to $[\text{Sr}/\text{Fe}] < -1.5$, and therefore was suggested to be a second generation star (Spite et al. 2000). The interesting pattern is that this binary shows almost solar Mg/Fe and Ca/Fe ratios, as would be the case with hypernovae. Another feature of CS22873-139 is enhanced Ti/Fe ($[\text{Ti}/\text{Fe}] \sim +0.6$), which could be explained by an (especially, aspherical) hypernova explosion.

It has been pointed out that Ti is deficient in Galactic chemical evolution models using supernova yields currently available (e.g., Timmes et al. 1995; Thielemann et al. 1996), especially at $[\text{Fe}/\text{H}] \lesssim -1$ when SNe Ia have not contributed to the chemical evolution. However, if the contribution from hypernovae to Galactic chemical evolution is relatively large (or supernovae are more energetic than the typical value of 1×10^{51} erg), this problem could be relaxed. As we have seen in the previous section, the α -rich freezeout is enhanced in hypernovae because nucleosynthesis proceeds under the circumstance of lower densities and incomplete Si-burning occurs in more extended regions. Thus, ^{40}Ca , ^{44}Ca , and ^{48}Ti are produced and could be ejected into space more abundantly.

4.2. MANGANESE, CHROMIUM, COBALT

The observed abundances of metal-poor halo stars show quite interesting patterns. There are significant differences between the abundance patterns in the iron-peak elements below and above $[\text{Fe}/\text{H}] \sim -2.5$. For $[\text{Fe}/\text{H}] \lesssim -2.5$, the mean values of $[\text{Cr}/\text{Fe}]$ and $[\text{Mn}/\text{Fe}]$ decrease toward smaller metallicity, while $[\text{Co}/\text{Fe}]$ increases (McWilliam et al. 1995; Ryan et al. 1996). This trend cannot be explained with the conventional chemical evolution model that uses previous nucleosynthesis yields.

Mass Cut Dependence. Nakamura et al. (1999) have shown that this trend of decreasing Cr and Mn with increasing Co is reproduced

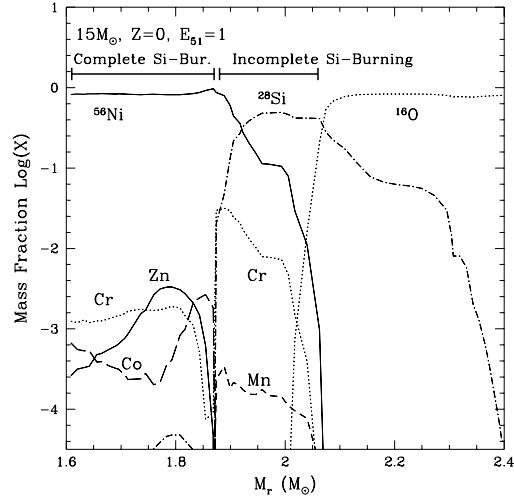


Figure 8 Abundance distribution just after supernova explosion for the Pop III model with mass $15M_{\odot}$. The lines labeled by Cr, Mn, Co and Zn actually indicate unstable ^{52}Fe , ^{55}Co , ^{59}Cu , and ^{64}Ge , respectively, which eventually decay to the labeled elements (Umeda & Nomoto 2001).

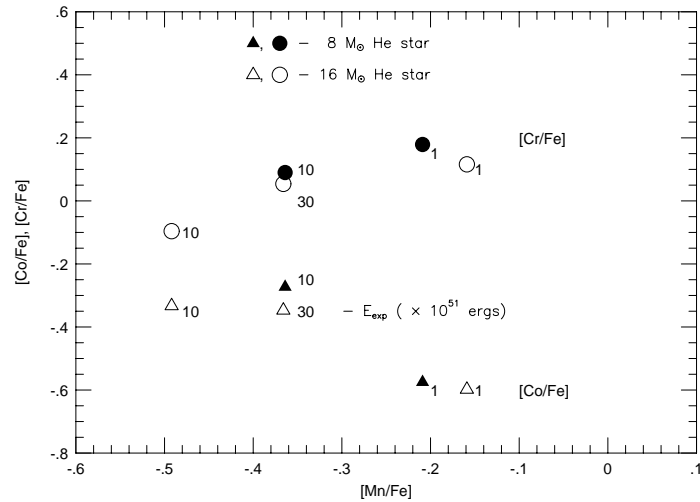


Figure 9 $[\text{Mn}/\text{Fe}]$ vs. $[\text{Co}/\text{Fe}]$ and $[\text{Cr}/\text{Fe}]$ for the $40 M_{\odot}$ star ($16 M_{\odot}$ He star) models with $E = (1.0 - 30) \times 10^{51}$ ergs, and the $25 M_{\odot}$ star ($8 M_{\odot}$ He star) models with $E = (1 - 10) \times 10^{51}$ ergs (Nakamura et al. 2001b).

by decreasing the mass cut between the ejecta and the collapsed star for the same explosion model. This is because Co is mostly produced in complete Si-burning regions, while Mn and Cr are mainly produced in the outer incomplete Si-burning region (Fig. 8). If the mass cut is located at smaller M_r , the mass ratio between the complete and incomplete Si-burning region is larger. Therefore, mass cuts at smaller M_r increase the Co fraction but decrease the Mn and Cr fractions in the ejecta. Nakamura et al. (1999) have also shown that the observed trend with respect to $[\text{Fe}/\text{H}]$ may be explained if the mass cut tends to be smaller in M_r for the larger mass progenitor.

Energy Dependence. Nakamura et al. (2001b) have investigated whether the observed trend of these iron-peak elements in metal-poor stars can be explained with the abundance pattern of hypernovae. In Figure 9, we plot $[\text{Mn}/\text{Fe}]$ vs. $[\text{Co}/\text{Fe}]$ and $[\text{Cr}/\text{Fe}]$ for the 16 M_\odot He star models with $E = (1 - 30) \times 10^{51}$ ergs, and 8 M_\odot He star models with $E = (1 - 10) \times 10^{51}$ ergs. This figure clearly shows the correlation between $[\text{Mn}/\text{Fe}]$ and $[\text{Cr}/\text{Fe}]$, and anti-correlation between $[\text{Mn}/\text{Fe}]$ and $[\text{Co}/\text{Fe}]$, which are the same trends as observed in the metal-poor stars.

To understand the dependence on E , let us compare the models with 1×10^{51} and 10×10^{51} ergs which have almost the same mass cut. In the model with $E = 10 \times 10^{51}$ ergs, both complete and incomplete Si-burning regions shift outward in mass compared with $E = 1 \times 10^{51}$ ergs because of a larger explosion energy. Thus, the model with larger E has a larger mass ratio between the complete and incomplete Si-burning regions. (This relation between E and the mass ratio does not hold if the explosion energy is too large, because incomplete Si-burning extends so far out that Mn and Cr increase too much to fit the metal-poor star data.)

In metal-poor stars, $[\text{Mn}/\text{Fe}]$ increases with $[\text{Fe}/\text{H}]$. Hypernova yields are consistent with this trend if hypernovae with larger E induce the formation of stars with smaller $[\text{Fe}/\text{H}]$. This supposition is reasonable because the mass of interstellar hydrogen gathered by a hypernova is roughly proportional to E (Cioffi et al. 1988; Shigeyama & Tsujimoto 1998) and the ratio of the ejected iron mass to E is smaller for hypernovae than for canonical supernovae.

4.3. ZINC

For Zn, early observations have shown that $[\text{Zn}/\text{Fe}] \sim 0$ for $[\text{Fe}/\text{H}] \simeq -3$ to 0 (Snedden, Gratton, & Crocker 1991). Recently Primas et al. (2000) have suggested that $[\text{Zn}/\text{Fe}]$ increases toward smaller metallicity

as seen in Figure 10, and Blake et al. (2001) has one with $[\text{Zn}/\text{Fe}] \simeq 0.6$ at $[\text{Fe}/\text{H}] = -3.3$ (see Ryan 2001).

As for Zn, its main production site has not been clearly identified. If it is mainly produced by s-processes, the abundance ratio $[\text{Zn}/\text{Fe}]$ should decrease with $[\text{Fe}/\text{H}]$. This is not consistent with the observations of $[\text{Zn}/\text{Fe}] \sim 0$ for $[\text{Fe}/\text{H}] \simeq -2.5$ to 0 and the increase in $[\text{Zn}/\text{Fe}]$ toward lower metallicity for $[\text{Fe}/\text{H}] \lesssim -2.5$. Another possible site of Zn production is SNe II. However, previous nucleosynthesis calculations in SNe II appears to predict decreasing Zn/Fe ratio with Fe/H (Woosley & Weaver 1995; Goswami & Prantzos 2000).

Understanding the origin of the variation in $[\text{Zn}/\text{Fe}]$ is very important especially for studying the abundance of Damped Ly- α systems (DLAs), because $[\text{Zn}/\text{Fe}] = 0$ is usually assumed to determine their abundance pattern. In DLAs super-solar $[\text{Zn}/\text{Fe}]$ ratios have often been observed, but they have been explained that assuming dust depletion for Fe is larger than it is for Zn. However, recent observations suggest that the assumption $[\text{Zn}/\text{Fe}] = 0$ may not be always correct.

Spherical Hypernova Models. Umeda & Nomoto (2001) have calculated nucleosynthesis in massive Pop III stars and explored the parameter ranges ($M_{\text{cut}}(i)$, Y_e , M , and E) to reproduce $[\text{Zn}/\text{F}] \sim 0.5$ observed in extremely metal-poor stars. Their main results are summarized as follows.

1) The interesting trends of the observed ratios $[(\text{Zn}, \text{Co}, \text{Mn}, \text{Cr})/\text{Fe}]$ can be understood in terms of the variation of the mass ratio between the complete Si burning region and the incomplete Si burning region. The large Zn and Co abundances observed in very metal-poor stars are obtained if the mass-cut is deep enough, or equivalently if deep material from complete Si-burning region is ejected by mixing or aspherical effects. Vanadium also appears to be abundant at low $[\text{Fe}/\text{H}]$. Since V is also produced mainly in the complete Si-burning region, this trend can be explained in the same way as those of Zn and Co.

2) The mass of the incomplete Si burning region is sensitive to the progenitor mass M , being smaller for smaller M . Thus $[\text{Zn}/\text{Fe}]$ tends to be larger for less massive stars for the same E .

3) The production of Zn and Co is sensitive to the value of Y_e , being larger as Y_e is closer to 0.5, especially for the case of a normal explosion energy ($E_{51} \sim 1$).

4) A large explosion energy E results in the enhancement of the local mass fractions of Zn and Co, while Cr and Mn are not enhanced. This is because larger E produces larger entropy and thus more α -rich environment for α -rich freeze-out.

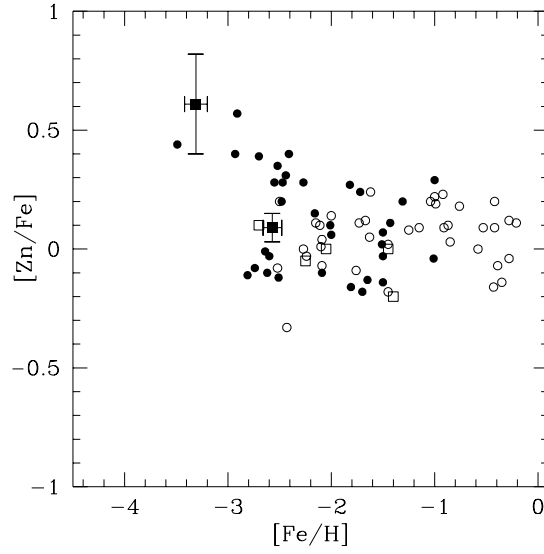


Figure 10 Observed abundance ratios of $[Zn/Fe]$. These data are taken from Primas et al. (2000) (filled circles), Blake et al. (2001) (filled square) and from Sneden et al. (1991) (others) (Umeda & Nomoto 2001).

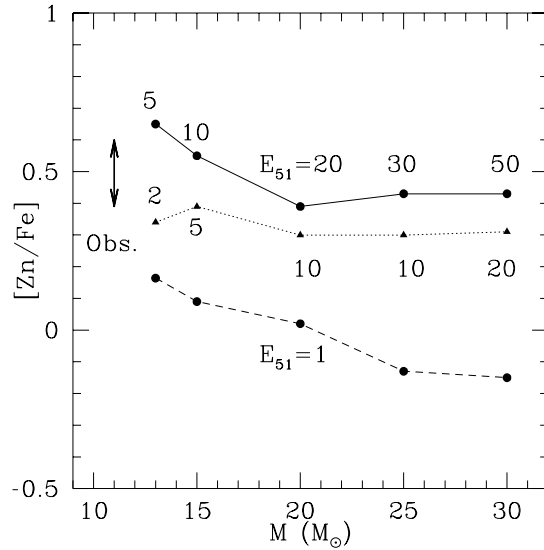


Figure 11 The maximum $[Zn/Fe]$ ratios as a function of M and E_{51} (Umeda & Nomoto 2001). The observed large $[Zn/Fe]$ ratio in very low-metal stars ($[Fe/H] < -2.6$) found in Primas et al. (2000) and Blake et al. (2001) are represented by a thick arrow.

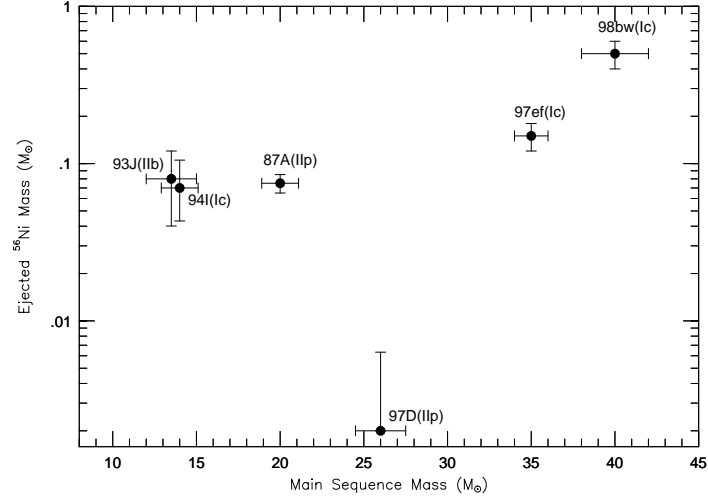


Figure 12 Ejected ^{56}Ni mass versus the main sequence mass of the progenitors of several bright supernovae obtained from light curve models (Iwamoto et al. 2000).

5) To be consistent with the observed $[\text{O}/\text{Fe}] \sim 0 - 0.5$ as well as with $[\text{Zn}/\text{Fe}] \sim 0.5$ in metal-poor stars, they propose that the “mixing and fall-back” process or aspherical effects are significant in the explosion of relatively massive stars.

The dependence of $[\text{Zn}/\text{Fe}]$ on M and E is summarized in Figure 11. They have found that models with $E_{51} = 1$ do not produce sufficiently large $[\text{Zn}/\text{Fe}]$. To be compatible with the observations of $[\text{Zn}/\text{Fe}] \sim 0.5$, the explosion energy must be much larger, i.e., $E_{51} \gtrsim 2$ for $M \sim 13M_{\odot}$ and $E_{51} \gtrsim 20$ for $M \gtrsim 20M_{\odot}$.

Observationally, the requirement of the large E might suggest that large M stars are responsible for large $[\text{Zn}/\text{Fe}]$, because E and M can be constrained from the observed brightness and light curve shape of supernovae as follows (Fig. 12). The recent supernovae 1987A, 1993J, and 1994I indicate that the progenitors of these normal SNe are 13 - 20 M_{\odot} stars and $E_{51} \sim 1 - 1.5$ (Nomoto et al. 1993, 1994; Shigeyama et al. 1994; Blinnikov et al. 2000). On the other hand, the masses of the progenitors of hypernovae with $E_{51} > 10$ (SNe 1998bw, 1997ef, and 1997cy) are estimated to be $M \gtrsim 25M_{\odot}$ (Nomoto et al. 2000; Iwamoto et al. 1998, 2000; Woosley et al. 1999; Turatto et al. 2000). This could be related to the stellar mass dependence of the explosion mechanisms and the formation of compact remnant, i.e., less massive stars form neutron stars, while more massive stars tend to form black holes.

To explain the observed relation between $[\text{Zn}/\text{Fe}]$ and $[\text{Fe}/\text{H}]$, we further need to know how M and E of supernovae and $[\text{Fe}/\text{H}]$ of metal-poor halo stars are related. In the early galactic epoch when the galaxy is not yet chemically well-mixed, $[\text{Fe}/\text{H}]$ may well be determined by mostly a single SN event (Audouze & Silk 1995). The formation of metal-poor stars is supposed to be driven by a supernova shock, so that $[\text{Fe}/\text{H}]$ is determined by the ejected Fe mass and the amount of circumstellar hydrogen swept-up by the shock wave (Ryan et al. 1996).

Explosions with the following two combinations of M and E can be responsible for the formation of stars with very small $[\text{Fe}/\text{H}]$:

i) Energetic explosions of massive stars ($M \gtrsim 25M_{\odot}$): For these massive progenitors, the supernova shock wave tends to propagate further out because of the large explosion energy and large Strömgren sphere of the progenitors (Nakamura et al. 1999). The effect of E may be important since the hydrogen mass swept up by the supernova shock is roughly proportional to E (e.g., Ryan et al 1996; Shige-yama & Tsujimoto 1998).

ii) Normal supernova explosions of less massive stars ($M \sim 13M_{\odot}$): These supernovae are assumed to eject a rather small mass of Fe (Shige-yama & Tsujimoto 1998), and most SNe are assumed to explode with normal E irrespective of M .

The above relations lead to the following two possible scenarios to explain $[\text{Zn}/\text{Fe}] \sim 0.5$ observed in metal-poor stars.

i) Hypernova-like explosions of massive stars ($M \gtrsim 25M_{\odot}$) with $E_{51} > 10$: Contribution of highly asymmetric explosions in these stars may also be important. The question is what fraction of such massive stars explode as hypernovae; the IMF-integrated yields must be consistent with $[\text{Zn}/\text{Fe}] \sim 0$ at $[\text{Fe}/\text{H}] \gtrsim -2.5$.

ii) Explosion of less massive stars ($M \lesssim 13M_{\odot}$) with $E_{51} \gtrsim 2$ or a large asymmetry: This scenario, after integration over the IMF, can reproduce the observed abundance pattern for $[\text{Fe}/\text{H}] \gtrsim -2$. However, the Fe yield has to be very small in order to satisfy the observed $[\text{O}/\text{Fe}]$ value ($\gtrsim 0.5$) for the metal-poor stars. For example, the ^{56}Ni mass yield of our $13M_{\odot}$ model has to be less than $0.006M_{\odot}$, which appears to be inconsistent with the nearby SNe II observations.

It seems that the $[\text{O}/\text{Fe}]$ ratio of metal-poor stars and the E - M relations from supernova observations (Fig. 12) favor the massive energetic explosion scenario for enhanced $[\text{Zn}/\text{Fe}]$. However, we need to construct detailed galactic chemical evolution models to distinguish between the two scenarios for $[\text{Zn}/\text{Fe}]$.

Aspherical Hypernova Models. Iron-peak elements are produced in the deep region near the mass cut, so that their production is

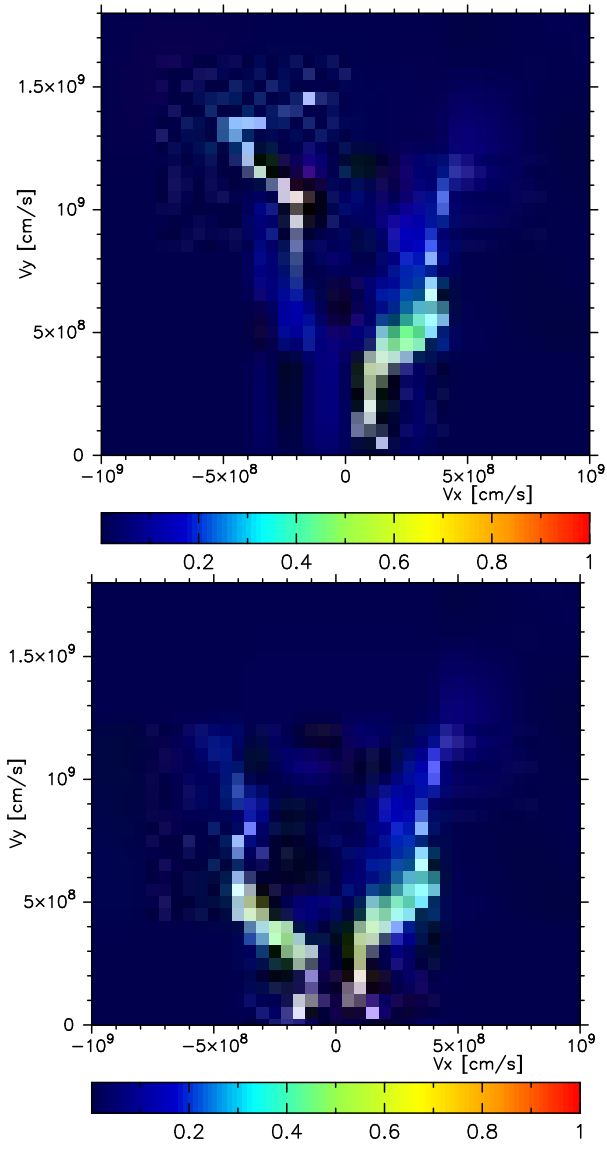


Figure 13 The density distributions of Zn (top: left half) and Fe (top: right half) and that of Mn (bottom: left half) and Fe (bottom: right half). The densities of each element are represented with linear scale, from 0 to the max density of each element (Maeda 2001).

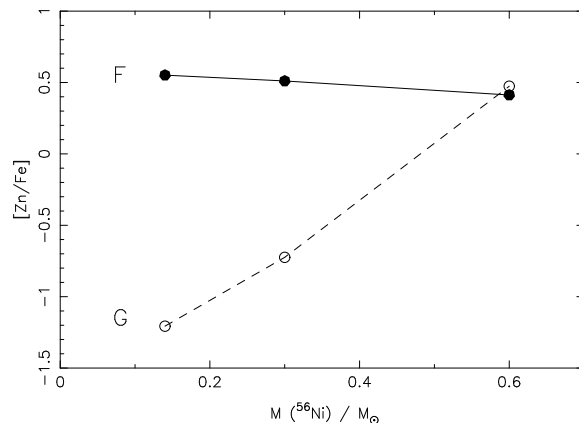


Figure 14 $[\text{Zn}/\text{Fe}]$ as a function of the mass of ejected ^{56}Ni (Maeda 2001). Larger ^{56}Ni mass corresponds to deeper mass cut. The filled and open circles denote the aspherical and spherical models, respectively. The progenitor is the $40M_{\odot}$ star (Umeda & Nomoto 2001).

strongly affected by asphericity of an explosion. Figure 13 shows the 2D density distribution of ^{64}Ge (which decays into ^{64}Zn) and that of ^{55}Co (which decays into ^{55}Mn). ^{64}Zn , which is produced by the strong α -rich freezeout, is distributed preferentially in the z -direction. Moreover, ^{64}Zn production is strongly enhanced compared with a spherical model, since the post-shock temperature along the z -direction is much higher than that of a spherical model. On the other hand, ^{55}Mn , which is produced by incomplete silicon burning, surrounds ^{56}Fe and located preferentially in the r -direction. Accordingly, materials with higher $[\text{Zn}/\text{Fe}]$ and lower $[\text{Mn}/\text{Fe}]$ are ejected along the Z -direction with higher velocities, and materials with lower $[\text{Zn}/\text{Fe}]$ and higher $[\text{Mn}/\text{Fe}]$ are ejected toward the r -direction with lower velocities.

Figure 14 shows that $[\text{Zn}/\text{Fe}]$ is larger for deeper mass cut (i.e., larger ^{56}Ni mass) for spherical explosion, while $[\text{Zn}/\text{Fe}] \sim 0.5$ is realized irrespective of the mass cut. This comes from the difference in the site of the Zn production. In the spherical case, Zn is produced only in the deepest layer, while in the aspherical model, the complete silicon burning region is elongated to the z (jet) direction (Figure 13), so that $[\text{Zn}/\text{Fe}]$ is enhanced irrespective of the mass cut.

In this way, larger asphericity in the explosion leads to larger $[\text{Zn}/\text{Fe}]$ and $[\text{Co}/\text{Fe}]$, but to smaller $[\text{Mn}/\text{Fe}]$ and $[\text{Cr}/\text{Fe}]$. Then, if the degree of the asphericity tends to be larger for lower $[\text{Fe}/\text{H}]$, the trends of $[\text{Zn}$, Co , Mn , $\text{Cr}/\text{Fe}]$ follow the observed ones.

It is likely that in the real situations, the asphericity, mixing, and the effects of the mass-cut (Nakamura et al. 1999) work to make observed trends. Then, the restrictions encountered by each of them (e.g., requirement of large Y_e , large amounts of mixing) may be relaxed.

5. OTHER OBSERVATIONAL SIGNATURES OF HYPERNOVA NUCLEOSYNTHESIS

5.1. STARBURST GALAXIES

X-ray emissions from the starburst galaxy M82 were observed with ASCA and the abundances of several heavy elements were obtained (Tsuru et al. 1997). Tsuru et al. (1997) found that the overall metallicity of M82 is quite low, i.e., O/H and Fe/H are only 0.06 - 0.05 times solar, while Si/H and S/H are $\sim 0.40 - 0.47$ times solar. This implies that the abundance ratios are peculiar, i.e., the ratio O/Fe is about solar, while the ratios of Si and S relative to O and Fe are as high as $\sim 6 - 8$. These ratios are very different from those ratios in SNe II. The age of M82 is estimated to be $\lesssim 10^8$ years, which is too young for Type Ia supernovae to contribute to enhance Fe relative to O. Tsuru et al. (1997) also estimated that the explosion energy required to produce the observed amount of hot plasma per oxygen mass is significantly larger than that of normal SNe II (here the oxygen mass dominates the total mass of the heavy elements). Tsuru et al. (1997) thus concluded that neither SN Ia nor SN II can reproduce the observed abundance pattern of M82.

Compared with normal SNe II, the important characteristic of hypernova nucleosynthesis is the large Si/O, S/O, and Fe/O ratios. Figure 15 shows the good agreement between the hypernova model and the observed abundances in M82 (Umeda et al. 2001). Hypernovae could also produce larger E per oxygen mass than normal SNe II. We therefore suggest that hypernova explosions may make important contributions to the metal enrichment and energy input to the interstellar matter in M82. If the IMF of the star burst is relatively flat compared with Salpeter IMF, the contribution of very massive stars and thus hypernovae could be much larger than in our Galaxy.

5.2. BLACK HOLE BINARIES

X-ray Nova Sco (GRO J1655-40), which consists of a massive black hole and a low mass companion (e.g., Brandt et al. 1995; Nelemans et al. 2000), also exhibits what could be the nucleosynthesis signature of a hypernova explosion. The companion star is enriched with Ti, S, Si,

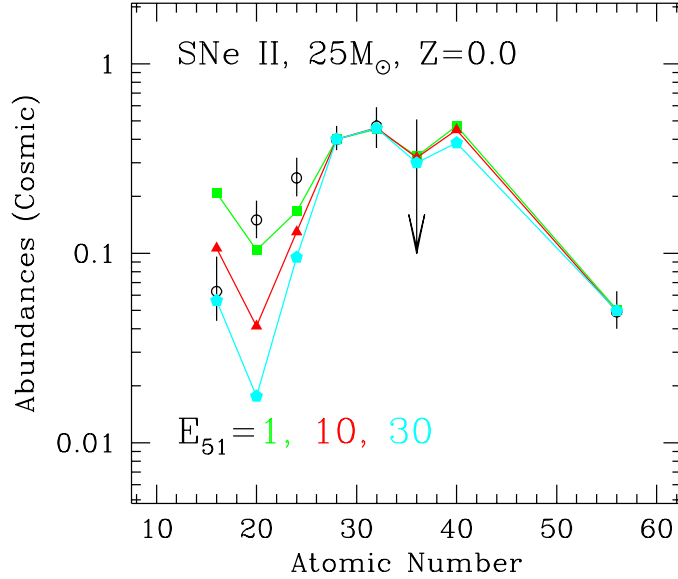


Figure 15 Abundance patterns in the ejecta of $25M_{\odot}$ metal-free SN II and hypernova models compared with abundances (relative to the solar values) of M82 observed with ASCA (Tsuru et al. 1997). Here, the open circles with error bars show the M82 data. The filled square, triangle, and pentagons represent $E_{51}=1, 10,$ and 30 models, respectively, where E_{51} is the explosion energy in 10^{51} ergs. Theoretical abundances are normalized to the observed Si data, and the mass cuts are chosen to eject $0.07, 0.095,$ and $0.12 (M_{\odot})$ Fe for $E_{51} = 1, 10,$ and 30 , respectively (Umeda et al. 2001).

Mg, and O but not much Fe (Israelian et al. 1999). This is compatible with heavy element ejection from a black hole progenitor. In order to eject large amount of Ti, S, and Si and to have at least $\sim 4 M_{\odot}$ below mass cut and thus form a massive black hole, the explosion would need to be highly energetic (Figure 1; Israelian et al. 1999; Brown et al. 2000; Podsiadlowski et al. 2001). A hypernova explosion with the mass cut at large M_r ejects a relatively small mass Fe and would be consistent with these observed abundance features.

Alternatively, if the explosion which resulted from the formation of the black hole in Nova Sco was asymmetric, then it is likely that the companion star captured material ejected in the direction away from the strong shock which contained relatively little Fe compared with the ejecta in the strong shock (Maeda et al. 2000).

6. SUMMARY AND DISCUSSION

We investigated explosive nucleosynthesis in hypernovae. Detailed nucleosynthesis calculations were performed for both spherical and aspherical explosions. We also studied implications to Galactic chemical evolution and the abundances in metal-poor stars. The characteristics of hypernova yields compared to those of ordinary core-collapse supernovae are summarized as follows:

1) Complete Si-burning takes place in more extended region, so that the mass ratio between the complete and incomplete Si burning regions is generally larger in hypernovae than normal SNe II. As a result, higher energy explosions tend to produce larger $[(\text{Zn}, \text{Co})/\text{Fe}]$, small $[(\text{Mn}, \text{Cr})/\text{Fe}]$, and larger $[\text{Fe}/\text{O}]$. If hypernovae made significant contributions to the early Galactic chemical evolution, it could explain the large Zn and Co abundances and the small Mn and Cr abundances observed in very metal-poor stars. The large $[\text{Fe}/\text{O}]$ observed in some metal-poor stars and galaxies might possibly be the indication of hypernovae rather than Type Ia supernovae.

2) In hypernovae, Si-burning takes place in lower density regions, so that the effects of α -rich freezeout is enhanced. Thus ^{44}Ca , ^{48}Ti , and ^{64}Zn are produced more abundantly than in normal supernovae. The large $[(\text{Ti}, \text{Zn})/\text{Fe}]$ ratios observed in very metal poor stars strongly suggest a significant contribution of hypernovae.

3) Oxygen burning also takes place in more extended regions for the larger explosion energy. Then a larger amount of Si, S, Ar, and Ca ("Si") are synthesized, which makes the Si/O ratio larger. The abundance pattern of the starburst galaxy M82, characterized by abundant Si and S relative to O and Fe, may be attributed to hypernova explosions if the IMF is relatively flat, and thus the contribution of massive stars to the galactic chemical evolution is large.

More direct signature of hypernovae can be seen in the black hole binary X-ray Nova Sco (GRO J1655-40), which indicates the production of a large amount of Ti, S, and Si when a massive black hole is formed as a compact remnant.

We also examine aspherical explosion models. The explosive shock is stronger in the jet-direction. The high explosion energies concentrated along the jet result in hypernova-like nucleosynthesis. On the other hand, the ejecta orthogonal to the jet is more like ordinary supernovae. Therefore, asphericity in the explosions strengthens the nucleosynthesis properties of hypernovae as summarized above in 1) and 2) but not 3).

It is shown that such a large Zn abundance as $[\text{Zn}/\text{Fe}] \sim 0.5$ observed in metal-poor stars can be realized in certain supernova models (Umeda

& Nomoto 2001). This implies that the assumption of $[\text{Zn}/\text{Fe}] \sim 0$ usually adopted in the DLA abundance analyses may not be well justified. Rather $[\text{Zn}/\text{Fe}]$ may provide important information on the IMF and/or the age of the DLA systems.

Properties of hypernova nucleosynthesis suggest that hypernovae of massive stars may make important contributions to the Galactic (and cosmic) chemical evolution, especially in the early low metallicity phase. This may be consistent with the suggestion that the IMF of Pop III stars is different from that of Pop I and II stars, and that more massive stars are abundant for Pop III (e.g., Nakamura & Umemura 1999; Omukai & Nishi 1999; Bromm, Coppi & Larson 1999).

Acknowledgments

We would like to thank P. Mazzali, N. Patat, S. Ryan, C. Kobayashi, M. Shirouzu, F. Thielemann for useful discussion. This work has been supported in part by the grant-in-Aid for Scientific Research (07CE2002, 12640233) of the Ministry of Education, Science, Culture, and Sports in Japan.

References

- Argast, D., Salmand, M., Gerhard, O.E., & Thielemann, F.-K. 2000, *A&A*, 356, 873
- Arnett, W. D., *Supernovae and Nucleosynthesis* (Princeton Univ. Press)
- Audouze, J., & Silk, J. 1995, *ApJ*, 451, L49
- Blake, L.A.J., Ryan, S.G., Norris, J.E., & Beers, T.C. 2001, *Nucl.Phys.A*.
- Blandford, R.D., & Znajek, R.L. 1977, *MNRAS*, 179, 433.
- Blinnikov, S., Lundqvist, P, Bartunov, O., Nomoto, K., & Iwamoto, K. 2000, *ApJ*, 532, 1132
- Branch, D. 2000, in “Supernovae and Gamma Ray Bursts” eds. M. Livio, et al. (Cambridge: Cambridge University Press), in press
- Brandt, W.N., Podsiadlowski, P., Sigurdssen, S. 1995, *MNRAS*, 277, L35
- Brown, G.E., Lee, C.-H., Wijers, R.A.M.J., Lee, H.K., Israelian, G., & Bethe, H.A. 2000, *New Astronomy*, 5, 191
- Bromm, V., Coppi, P.S., & Larson, R. B. 1999, *ApJ*, 527, L5
- Cappellaro, E., Turatto, M., & Mazzali, P. 1999, *IAU Circ.* 7091
- Cioffi, D.F., McKee, C.F. & Bertschinger, E. 1988, *ApJ*, 334, 252
- Danziger, I.J., et al. 1999, in *The Largest Explosions Since the Big Bang: Supernovae and Gamma Ray Bursts*, eds. M. Livio, et al. (STScI), 9
- Galama, T.J., et al. 1998, *Nature*, 395, 670
- Germany, L.M., Reiss, D.J., Schmidt, B.P., Stubbs, C.W., & Sadler, E.M. 2000, *ApJ*, 533, 320
- Hachisu, I., Matsuda, T., Nomoto, K., & Shigeyama, T. 1992, *ApJ*, 390, 230

- Hachisu, I., Matsuda, T., Nomoto, K., & Shigeyama, T. 1994, *A&AS*, 104, 341
- Hashimoto, M., Nomoto, K., & Shigeyama, T. 1989, *A&A*, 210, 5
- Höflich, P., Wheeler, J. C., & Wang, L., 1999, *ApJ*, 521, 179
- Israelian, G., Rebolo, R., Basri, G., Casares, J., & Martin E.L. 1999, *Nature*, 401, 142
- Iwamoto, K., et al. 1998, *Nature*, 395, 672
- Iwamoto, K., et al. 2000, *ApJ*, 534, 660
- Iwamoto, K., Nomoto, K., Höflich, P., Yamaoka, H., Kumagai, S., & Shigeyama, T., 1994, *ApJ*, 437, L115
- Khokhlov, A.M., Höflich, P.A., Oran, E.S., Wheeler, J.C., Wang, L., & Chtchelkanova, A.Yu. 1999, *ApJ*, 524, L107
- MacFadyen, A.I. & Woosley, S.E. 1999, *ApJ* 524, 262
- Maeda, K. 2001, Master Thesis, University of Tokyo
- Maeda, K., Nakamura, T., Nomoto, K., Mazzali, P.A., & Hachisu, I. 2000, *ApJ*, submitted (astro-ph/0011003)
- Mazzali, P.A., Iwamoto, K., & Nomoto, K. 2000, *ApJ*, 545, 407
- Mazzali, P.A., Nomoto, K., & Patat, F. 2001, *ApJ*, submitted
- McWilliam, A., Preston, G.W., Sneden, C., & Searle, L. 1995, *AJ*, 109, 2757
- Nagataki, S., Hashimoto, M., Sato, K., Yamada, S. 1997, *ApJ*, 486, 1026
- Nakamura, F., & Umemura, M. 1999, *ApJ*, 515, 239
- Nakamura, T. 1998, *Prog. Theor. Phys.*, 100, 921
- Nakamura, T., Mazzali, P. A., Nomoto, K., & Iwamoto, K. 2001a, *ApJ*, 550, 991
- Nakamura, T., Umeda, H., Iwamoto, K., Nomoto, K., Hashimoto, M., Hix, R.W., Thielemann, F.-K. 2001b, *ApJ*, 555, in press (astro-ph/0011184)
- Nakamura, T., Umeda, H., Nomoto, K., Thielemann, F.-K., & Burrows, A. 1999, *ApJ*, 517, 193
- Nelemans, G., Tauris, T.M., van den Heuvel, E.P.J. 2000, *A&A*, 352, 87
- Nomoto, K., Suzuki, T., Shigeyama, T., Kumagai, S., Yamaoka, H., Saio, H. 1993, *Nature*, 364, 507
- Nomoto, K., Yamaoka, H., Pols, O. R., van den Heuvel, E. P. J., Iwamoto, K., Kumagai, S., & Shigeyama, T. 1994, *Nature*, 371, 227
- Nomoto, K., & Hashimoto, M. 1988, *Phys. Rep.*, 256, 173
- Nomoto, K., et al. 2000, in “Supernovae and Gamma Ray Bursts” eds. M. Livio, et al. (Cambridge Univ. Press) (astro-ph/0003077)
- Omukai, K., & Nishi, R. 1999, *ApJ*, 518, 64
- Paczynski, B. 1998, *ApJ*, 494, L45
- Patat, F., et al. 2001, *ApJ*, in press (astro-ph/0103111)

- Podsiadlowski, Ph., Nomoto, K., Maeda, K., Nakamura, T., Mazzali, P.A., & Schmidt, B. 2001, in preparation
- Primas, F., Reimers, D., Wisotzki, L., Reetz, J., Gehren, T., & Beers, T.C. 2000, in *The First Stars*, ed. A. Weiss, et al. (Springer), 51
- Ryan, S.G. 2001, this volume
- Ryan, S.G., Norris, J.E. & Beers, T.C. 1996, *ApJ*, 471, 254
- Shigeyama, T., & Tsujimoto, T. 1998, *ApJ*, 507, L135
- Sollerman, J., Kozma, C., Fransson, C., Leibundgut, B., Lundqvist, P., Ryde, F., & Woudt, P. 2000, *ApJ* 537, L127
- Snedden, C., Gratton, R.G., & Crocker, D.A. 1991, *A&A*, 246, 354
- Spite, M., Depagne, E., Nordström, B., Hill, V., Cayrel, R., Spite, F., & Beers, T.C. 2000, *A&A*, 360, 1077
- Thielemann, F.-K., Nomoto, K., & Hashimoto, M. 1996, *ApJ*, 460, 408
- Tsujimoto, T., Nomoto, K., Yoshii, Y., Hashimoto, M., Yanagida, Y., & Thielemann, F.-K. 1995, *MNRAS*, 277, 945
- Tsuru, T. G., Awaki, H., Koyama K., Ptak, A. 1997, *PASJ*, 49, 619
- Turatto, et. al. 2000, *ApJ*, 534, L57
- Umeda, H., Nomoto, K. 2001, *ApJ*, submitted (astro-ph/0103241)
- Umeda, H., Nomoto, K. & Nakamura, T., 2000, in *The First Stars*, eds. A. Weiss, T. Abel & V. Hill (Berlin: Springer), 121
- Umeda, H., Nomoto, K. Tsuru, T., et al. 2001, in preparation
- Wheeler, J. C., Yi, I., Höflich, P. A., & Wang, L. 2000, *ApJ*, 537, 810
- Woosley, S.E. 1993, *ApJ*, 405, 273
- Woosley, S.E., Eastman, R.G., & Schmidt, B.P. 1999, *ApJ*, 516, 788
- Woosley, S. E., & Weaver, T. A. 1995, *ApJS*, 101, 181